Smart Structures and Systems, *Vol. 26*, *No. 6* (*2020*) *735-751*
DOI: https://doi.org/10.12989/sss.2020.26.6.735

Bayesian in-situ parameter estimation of metallic plates using piezoelectric transducers

Sina Asadi[1,2a], Mahnaz Shamshirsaz[*1] and Younes A. Vaghasloo[2b]

[1]*New Technologies Research Center, Amirkabir University of Technology (Tehran Polytechnic), No. 28, Alborz Ally, Hafez Ave, Tehran, Iran*
[2]*Department of Mechanical Engineering, Amirkabir University of Technology (Tehran Polytechnic), No. 350, Hafez Ave, Tehran, Iran*

(*Received February 22, 2020, Revised September 9, 2020, Accepted September 11, 2020*)

Abstract. Identification of structure parameters is crucial in Structural Health Monitoring (SHM) context for activities such as model validation, damage assessment and signal processing of structure response. In this paper, guided waves generated by piezoelectric transducers are used for in-situ and non-destructive structural parameter estimation based on Bayesian approach. As Bayesian approach needs iterative process, which is computationally expensive, this paper proposes a method in which an analytical model is selected and developed in order to decrease computational time and complexity of modeling. An experimental set-up is implemented to estimate three target elastic and geometrical parameters: Young's modulus, Poisson ratio and thickness of aluminum and steel plates. Experimental and simulated data are combined in a Bayesian framework for parameter identification. A significant accuracy is achieved regarding estimation of target parameters with maximum error of 8, 11 and 17 percent respectively. Moreover, the limitation of analytical model concerning boundary reflections is addressed and managed experimentally. Pulse excitation is selected as it can excite the structure in a wide frequency range contrary to conventional tone burst excitation. The results show that the proposed non-destructive method can be used in service for estimation of material and geometrical properties of structure in industrial applications.

Keywords: parameter estimation; guided wave; piezoelectric transducer; Bayesian analysis; non-destructive identification

1. Introduction

Modeling mechanical structures has a significant role in scientific and engineering achievements. Modeling makes describing complex phenomena feasible in a way that those phenomena can be well defined by mathematical rules (Shinozuka and Ghanem 1995). Identification of structure parameters is essential in many macro/micro scaled engineering fields. In micro scaled fields, several micromechanical models are available to estimate effective elastic properties such as rule of mixture, asymptotic homogenization, Halpin-Tsai method, Mori-Tanaka method and their variants (Şimşek *et al*. 2013, Attia *et al*. 2015, Liew *et al*. 2015, Arani and Kolahchi 2016, Akgöz and Civalek 2017, Ebrahimi *et al*. 2019, Civalek *et al*. 2020). In macro scaled scopes such as composite or functionally graded materials/structures, estimation of the effective mechanical properties is the first step of analysis and design (Vignoli *et al*. 2019).

In structural health monitoring as a macro scale field, identification of structure parameters is crucial for model validation and damage assessment (Xie *et al*. 2018). There are several challenges concerning uncertainties in material properties in SHM applications. One challenge is lack of information about physical properties of structure materials: conventional approximations based on engineering tables provided by manufacturers are not always reliable because of high diversity among specimens and arbitrary variable ranges. Using composite or complex materials in structures makes parameters of structure different from reported ones (Araujo *et al*. 2002). Second challenge is that most SHM equipment is installed on structures in operational phase of their life. Therefore, there is normally no prior data about their physical properties. Also, under operational loadings and various environmental conditions, physical properties of material may be changed (Morales-Valdez *et al*. 2018). These discrepancies between the material parameters used in mathematical or numerical models and their actual values might lead to excessive levels of deformation or vibration and consequently to a false diagnosis. Hence, knowing current values of material properties is of great importance (Yang *et al*. 2004, Gallina *et al*. 2017) and improves accuracy of damage characterization (detection, localization and quantification). On the other hand, most of SHM schemes need a reference state for intact structure which current state of structure can be compared to. Best choice for the reference state is the earliest time in structure life time. In practice, structure state at the start of service is the only choice as a reference, though defects which are result of manufacturing process are not considered in the reference state. Considering such defects needs a model that is in resemblance with the structure. This model makes

*Corresponding author, Professor,
E-mail: shamshir@aut.ac.ir
[a] Ph.D. Student, E-mail: s-asadi@aut.ac.ir
[b] Professor, E-mail: alizadeh@aut.ac.ir

Copyright © 2020 Techno-Press, Ltd.

ISSN: 1738-1584 (Print), 1738-1991 (Online)

damage detection of structure possible and provide information on quality of manufacturing process even before placing the structure in service (Pagnotta 2008, Zhang *et al*. 2016a, 2019); also, in the case of successful estimation of material parameters such as Young's modulus, an alternative nondestructive method is developed which can be used prior or alongside with destructive methods such as standard tensile test.

Though there are several methods for material characterization, there are only a few procedures that make identification of material properties possible in a nondestructive manner specially in plate-like structures with high accuracy (Gallina *et al*. 2017). Nondestructive parameter estimation methods are categorized into two main approaches: static and dynamic.

Digital Image Correlation (DIC) is one of most popular static techniques. It is a versatile method that provides a large amount of experimental data and allows covering a wide range of structure's surface (Zhang and Zhao 2013, Rahmatabadi *et al*. 2019, Cuadrado *et al*. 2020, Périé and Passieux 2020, Vijayanand *et al*. 2020). Dynamic approach has some advantages over static one: Specimens with much wider range of shapes and dimensions can be used in dynamic approach. Also, they lead to very precise measurements, nondestructively (Pagnotta 2008). Another remarkable feature concerning dynamic nondestructive parameter identification approach is that its outcome is valid on average for the examined part of specimen. Whereas parameters estimated by classical destructive or static (strain gauge-based) technique is limited and valid in a specific point of the test specimen (Araujo *et al*. 1996, 2000, 2002). Since dynamic methods of parameter identification are usually carried out at relatively low to medium frequency range, the corresponding wavelength is mostly above millimeter size. This renders that dynamic methods are best suited for macro scaled applications. In literature, dynamic approach is categorized into two main groups in the field of parameter and model identification: Wave propagation-based and vibration-based methods (Tam *et al*. 2017a). Vibration-based methods are mostly incorporating measured modal data such as natural frequency and mode shapes or kinematic parameters such as velocity and acceleration (Réthoré *et al*. 2013, Sanayei *et al*. 2015, Banerjee 2016, Oliveira *et al*. 2016, Battaglia *et al*. 2018). Wave-based approaches eliminate most restrictions of the vibration-based approaches. Specifically, they can be carried out at any frequency and do not require any knowledge of boundary conditions as it will be discussed in following sections (Ablitzer *et al*. 2014). The later advantage makes wave-based approaches suitable for specimens of various shapes, since there is no need to reduce specimens to a conventional/standard testing geometry. Parameter estimation using wave propagation can be applied in two ways (Vishnuvardhan *et al*. 2007a). One way: In situ reconstruction of essential parameters utilizing the leave-in-place transducers already integrated in the structure for SHM applications. This way, one could take advantage of existing transducers to estimate system parameters along with SHM system. Another way: Dedicated transducers are used as portable/embedded devices to reconstruct unknown essential parameters of the system during its service or as-fabricated structures. In wave-based approach, it is well known that ultrasonic bulk wave characteristics are insensitive to variation in some material properties. Moreover, using such waves, measurements in different directions are required to evaluate non-isotropic material properties. While using guided waves such as Rayleigh wave (Zhang *et al*. 2011, Lee *et al*. 2017) and Lamb wave (Pabisek and Waszczyszyn 2015, Gallina *et al*. 2017, Jia *et al*. 2019), only measurement in one direction is required to evaluate material properties in different directions (Vishnuvardhan e*t al*. 2007a, b). The most demanded parameter to be identified nondestructively is Young's modulus which is reported in literature consistently (Vishnuvardhan *et al*. 2007a, b, Hall and Michaels 2011, Ambrozinski *et al*. 2015, Lechleiter and Schlasche 2017, Tam *et al*. 2017b, Bales *et al*. 2018, Battaglia *et al*. 2018, Lu *et al*. 2018) since it is essential for both structural design and assessment of the structure performance. Prior knowledge of elastic constant is required in many fields: Structural health monitoring (Pant 2014), product lifecycle management (Gallina *et al*. 2017), active control applications (Pedersen *et al*. 2005, Araujo *et al*. 2009), composite laminas (Vishnuvardhan *et al*. 2007a, Ablitzer *et al*. 2014, Tam *et al*. 2017a, b, Battaglia *et al*. 2018, Lu *et al*. 2018), seismic exploration (Hall and Michaels 2011, Shirzad-Ghaleroudkhani *et al*. 2018), and algorithms: dispersion curve computation (Gallina *et al*. 2015, Pabisek and Waszczyszyn 2015), phase reconstruction (beam steering) (Vishnuvardhan *et al*. 2007b), time reversal (Agrahari and Kapuria 2016) and many others. Parameter identification can be achieved via deterministic techniques such as artificial neural networks (Pabisek and Waszczyszyn 2015), genetic algorithm (Liu *et al*. 2002, Vishnuvardhan *et al*. 2007b, Eremin *et al*. 2015, Bochud *et al*. 2018), least square method and its variants (Pollock *et al*. 2014, Auzins and Skukis 2015, Xu *et al*. 2020) or stochastic techniques including Kalman filter (Ebrahimian *et al*. 2015, Olivier and Smyth 2018, Sen and Bhattacharya 2018), particle filter (Słoński 2014, Murakami *et al*. 2018) and Bayesian framework which will is addressed in this paper. Each of these techniques can be merged with mathematical tools based on signals which are collected from structure such as Short-Time Fourier Transform (STFT) (Nevaranta *et al*. 2015), wavelet transform (Zhang *et al*. 2016a, Lee *et al*. 2017, Pirboudaghi *et al*. 2018), chirplet transform (Deng *et al*. 2016).

Of the recent studies concerning mechanical properties identification, Webersen *et al*. (2018) used laser-induced ultrasonic Lamb waves and piezo-ceramic strip transducer as actuator and sensor respectively (Webersen *et al*. 2018). They used a wave number-based cost function and a simplex algorithm to minimize the cost function to estimate elastic constants (Young and shear modulus and Poisson ratio in different directions) in a continuous-fiber reinforced thermoplastic plates. Battaglia *et al*. (2018) implemented a Particle Swarm Optimization (PSO) on a Rayleigh-Ritz approach driven natural frequencies and mode shapes to identify mechanical properties of orthotropic plates (Battaglia *et al*. 2018). They used a laser scanning

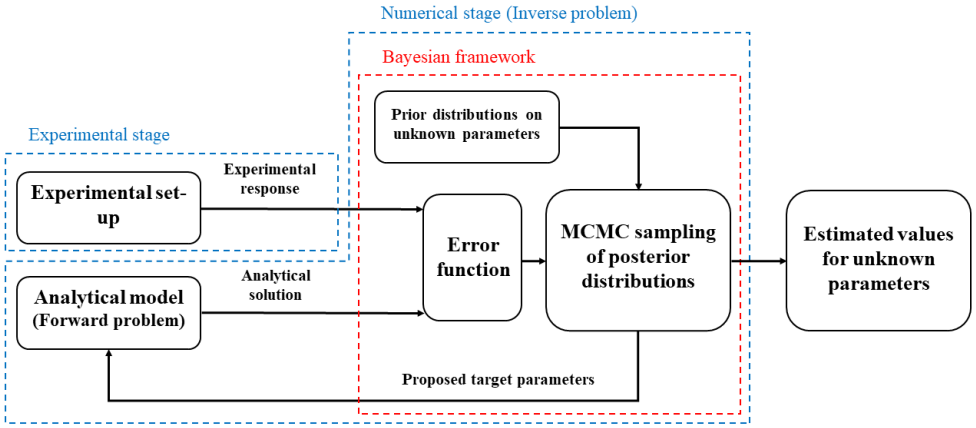

Fig. 1 Methodology structure proposed and followed in the study

vibrometer to measure velocity and displacement in the vibrating plate based on free-vibration conditions. Bales et al. proposed a Bayesian frame work to characterize anisotropic elastic properties and crystallographic orientation of two titanium and nickel based alloys using resonance frequencies collected via Resonance Ultrasound Spectroscopy (RUS). Gallina *et al*. (2017) also presented a Bayesian approach for elastic constants such as Young's modulus and material properties such as thickness and density identification in thin orthotropic composite plates (Gallina *et al*. 2017). They studied Lamb wave propagation and the related dispersion curves measured by a scanning laser Doppler vibrometer, experimentally. In most of previous research works, characterization of mechanical parameter is carried out using complex experimental set-ups limiting its application in industry.

Most studies incorporating Bayesian framework for elastic and geometrical parameter estimation use numerical models such as finite element. This is the main reason why Bayesian approaches have not been widely spread in mechanical engineering filed. Despite advantages numerical modeling offers, it has major drawbacks which are computational cost and time of solution. In this study an analytical solution based on 3D linear elasticity for modeling propagation of Lamb waves is implemented. Such analytical modeling makes iterative solution of wave propagation possible which has a central role in Bayesian estimation. However, using analytical modeling introduces limitation that should be addressed. In the analytical model it is assumed that plate is infinite and therefore no reflected wave from boundaries exists. Since the error function which will be used in the next sections compares experimental and analytical responses, reflection from boundaries should be removed from experimental response. In present paper a novel procedure is proposed to manage such reflected waves.

The main purpose of this study is to examine the reliability of proposed non-destructive method based on Lamb waves for estimation of mechanical and geometrical properties such as Young's modulus, Poisson ratio and thickness of isotropic plates. In process of achieving this goal, other parameters can be also estimated by construction. Main contribution of present study is attributed to utilizing just piezoelectric transducers to identify mechanical properties of metallic plates non-destructively. Corresponding electrical signals are measured with a simple data acquisition unit. This is contrary to other techniques using rather expensive and complicated set-ups and devices. Proposed procedure significantly reduces cost and complexity of identification process.

The paper is structured as follows. First, forward problem is discussed and effective parameters on the forward problem are addressed. A sensitivity analysis is performed to point out parameters with the most influence on structure response. Then, introduction to Bayesian framework is presented in which Gibbs sampler is used to sample posterior marginal distribution of unknown parameters. Experimental set-up and specimens are explained in the next section. Finally, results of proposed estimation framework are presented and accuracy of estimated parameter are reported.

2. Methods

Most of parameter estimation schemes for plate-like structures use deterministic approaches which provide only point estimate for unknown parameters regardless of results precision (Bales *et al*. 2018). This means there is no information about how well the unknown parameters are identified. Also, they often lack a procedure to characterize estimation uncertainty systematically (Słoński 2014). Though model-based deterministic optimization has extensively been used in parameter identification studies, it is stated by several authors that a stochastic treatment of such problems yields to more robust results (Gogu *et al*. 2010, Ma *et al*. 2014, Warner and Hochhalter 2016). Sources of uncertainties include uncertainty of unknown parameters, limited knowledge about mathematical model of structure and variability raised from experimental measurements error. In this context, parameter estimation methods based on Bayesian inference offer a very powerful framework with systematic uncertainty quantification as it is able to account for all stated uncertainty sources (Yuen and Ortiz 2018). The importance of Bayesian methods has increased rapidly over the last decade. This is invigorated

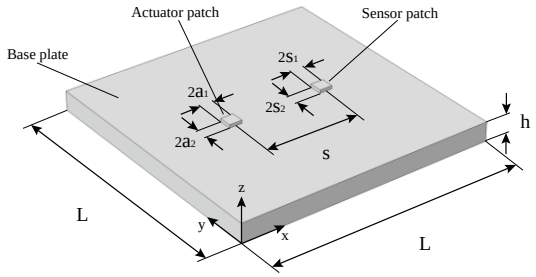

Fig. 2 Schematic of plate equipped with piezoelectric transducers as actuator and sensor with dimensions

by understanding of the advantages that Bayesian inference entails. It allows more accurate representation of experimental uncertainty as well as a way to incorporate the prior information, often exists before carrying out experimental tests. The usage of prior information regularizes the identification problems which is commonly ill-conditioned in presence of small amount of experimental data (Gallina *et al*. 2017, Erazo and Nagarajaiah 2018). A Bayesian approach does not yield point solutions but a collection of highly plausible results which are in best agreement with initial knowledge and new provided data from experiment (Argyris *et al*. 2018). So, Bayesian results are more informative than deterministic optimization. Moreover, a Bayesian framework is also more robust to isolated (local) optima which may not have a physical explanation but are originated from numerical error. One other worthwhile aspect of Bayesian approach is that it is sequential; it makes identification problems be solved recursively which improves results any time that new evidence is available.

In this section, a Bayesian framework to non-destructively estimate mechanical properties of a metallic plate is described. Bayesian based method proposed in this study, to estimate target parameters, is composed of several stages which are shown in Fig. 1.

2.1 Forward problem: Analytical model

Most parameter estimation methods come down to an optimization problem and solving such problems is usually iterative. Thus, for forward problem (relating mathematical model to observed data, assuming known model parameters), it is required to be solved repeatedly. Hence, solution time of forward problem takes up much of overall time in parameter estimation procedure and it should be as short as possible. There are several methods for solving a wave propagation problem including analytical (Giurgiutiu 2005, Raghavan and Cesnik 2005, Lechleiter and Schlasche 2017, Battaglia *et al*. 2018), numerical (Ge *et al*. 2014, Ambrozinski *et al*. 2015, Gallina *et al*. 2015, Lu *et al*. 2018) and semi-analytical (Shen and Giurgiutiu 2016, Zou and Aliabadi 2017) approaches. Each method has its benefits which is problem dependent. Due to reasons mentioned earlier, in this study choosing a method with minimum solution time is advantageous since forward problem has to be solved repeatedly. Among solving methods, analytical methods have the shortest time. However, their accuracy and applicability are limited especially for geometrically complex problems. Parameter estimation schemes based on dispersion curves, require signals of several points away from excitation source to calculate dispersion curves (Gallina *et al*. 2015, 2017, Pabisek and Waszczyszyn 2015). This increases number of transducers required to excite the structure and measure response. Modeling piezoelectric sensor and actuator makes experimental part of parameter estimation process much simpler since only voltage signals are recorded from piezoelectric transducers installed on the structure. This is contrary to other methods which require special measurement devices to measure quantities such as displacement, acceleration, etc.

In this study, analytical modeling of wave propagation in plate is developed based on Raghavan and Cesnik work (Raghavan and Cesnik 2005) in which, anti-symmetric part of solution was not reported in the original work and it is developed in present paper. This procedure provides enough accuracy for wave propagation modeling while keeping solution time minimum. Wave propagation modeling is based on 3D linear elasticity for isotropic plates and it is capable of considering arbitrary shape finite-dimensional surface-bonded piezoelectric wafer actuator and sensor. In this study, rectangular shaped sensor and actuator and ideal bonding between piezoelectric patches and base structure are assumed. Fig. 2 shows a metallic plate with two rectangular piezoelectric actuator and sensor according to a Cartesian coordinate system.

Guided waves generated by the actuator, are picked up by sensor after traveling distance s. Voltage which is induced on the sensor by incident wave is defined in Eqs. (1)-(2) for symmetric and antisymmetric parts of propagated wave

$$V^{S}_{Sensor}(t) = \sum_{\xi^S} \frac{-8\tau_0 Y_c^{11} h_c g_{31}}{\pi\mu s_1 s_2 (1-\nu_c)} \frac{N_s(\xi^S)}{(\xi^S)^2 D'_S(\xi^S)} e^{i\omega t} \times \int_0^{\frac{\pi}{2}} \{[\sin(\xi^S a_1 cos\gamma)\sin(\xi^S a_2 sin\gamma)\sin(\xi^S s_1 cos\gamma) \sin(\xi^S s_2 sin\gamma)] \times [sin^2 2\gamma]^{-1}\} \times e^{-i\xi^S(x_c cos\gamma + y_c sin\gamma)} d\gamma \quad (1)$$

$$V^{A}_{Sensor}(t) = \sum_{\xi^A} \frac{-8\tau_0 Y_c^{11} h_c g_{31}}{\pi\mu s_1 s_2 (1-\nu_c)} \frac{N_A(\xi^A)}{(\xi^A)^2 D'_A(\xi^A)} e^{i\omega t} \times \int_0^{\frac{\pi}{2}} \{[\sin(\xi^A a_1 cos\gamma)\sin(\xi^A a_2 sin\gamma)\sin(\xi^A s_1 cos\gamma) \sin(\xi^A s_2 sin\gamma)] \times [sin^2 2\gamma]^{-1}\} \times e^{-i\xi^A(x_c cos\gamma + y_c sin\gamma)} d\gamma \quad (2)$$

where Y_c^{11}, ν_c, h_c and g_{31} are in-plane Young's modulus, Poisson ratio, thickness and piezoelectric constant of the piezoelectric material, respectively. a_1, a_2 and s_1, s_2 are half length of actuator and sensor length and width. Moreover, x_c, y_c are relative position of middle points of sensor to actuator along in-plane *x*-*y* coordinates, respectively. ω and t are circular frequency and time. ξ is wavenumber defined as ω/c in which c is wave speed. D is characteristic equation obtained separately for symmetric and antisymmetric motions as

$$\begin{aligned} D_S(\xi^S) &= ((\xi^S)^2 - q^2)^2\, cos(pd)\, sin(qd) \\ &\quad + 4pq(\xi^S)^2\, sin(pd)\, cos(qd) \\ D_A(\xi^A) &= ((\xi^A)^2 - q^2)^2\, sin(pd)\, cos(qd) \\ &\quad + 4pq(\xi^A)^2\, cos(pd)\, sin(qd) \end{aligned} \tag{3}$$

which accepts eigenvalues ξ^S and ξ^A for symmetric and anti-symmetric modes, respectively. D' is derivative of D with respect to ξ. Also, following procedure described in (Raghavan and Cesnik 2005) gives definition of N for symmetric and antisymmetric modes as

$$\begin{aligned} N_S(\xi^S) &= q\xi^S((\xi^S)^2 + q^2)\, cos(pd)\, cos(qd) \\ N_A(\xi^A) &= q\xi^A((\xi^A)^2 + q^2)\, sin(pd)\, sin(qd) \end{aligned} \tag{4}$$

where p and q are defined as

$$\begin{aligned} p^2 &= \frac{\omega^2}{c_p^2} - \xi^2, \qquad q^2 = \frac{\omega^2}{c_s^2} - \xi^2 \\ c_p^2 &= \frac{\lambda + 2\mu}{\rho}, \qquad c_s^2 = \frac{\mu}{\rho} \end{aligned} \tag{5}$$

c_p and c_s are pressure (longitudinal) and shear (transverse) wave speeds, λ and μ are the Lame first and second constants, ρ and d are mass density and half the thickness for plate structure h. τ_0 is called interfacial shear stress causing in-plane traction of uniform magnitude along transducers perimeters (Giurgiutiu 2005). It is the connection between actuator/sensor and the structure and proportional to the Induced-Strain Actuation (ISA) in the piezoelectric patch by the electric voltage, defined as (Giurgiutiu 2007)

$$\varepsilon_{\mathrm{ISA}}(t) = d_{31}E_3(t) = \frac{d_{31}v(t)}{h_c} \tag{6}$$

where d_{31} and v are piezoelectric coefficient and excitation voltage. Index 3 is normal direction of the piezoelectric patch on which voltage is applied and index 1 demonstrates in-plane direction. Combining Eqs. (1)-(2) gives voltage signal on sensor due to received propagated wave as

$$v_{Sensor}(t) = v^S_{Sensor}(t) + v^A_{Sensor}(t) \tag{7}$$

In development of sensor voltage equation, it is assumed that all the frequencies contributing in wave generation, have magnitude of 1, i.e., all frequencies have same contribution in power spectrum of excitation. This means interfacial shear stress τ_0 is constant for all values of ξ. In the case where voltage response to desired excitation is being sought, one should take Fourier transform of τ_0. Since only ε_{ISA} is time dependent, taking Fourier transform of Eq. (6) gives

$$E_{ISA}(\omega) = \frac{d_{31}V(\omega)}{h_c} \tag{8}$$

where E_{ISA} and V are Fourier transformed versions of ε_{ISA} and v. Thus, to evaluate response to any arbitrary excitation, first it is transformed into frequency domain, then its corresponding component at each frequency, is inserted into Eq. (7) using interfacial shear stress relation and Eq. (8).

2.2 Unknown parameters

Generally, each physical or geometrical quantity contributing in mathematical model can be considered as unknown parameter. However, there are some remarks that are necessary to be highlighted. From the mathematical viewpoint, parameter estimation procedure leads to an optimization problem wherein the procedure can become very costly in terms of computational time and complexity when the set of unknown parameters increases, which is likely to be the case. If the model response is sensitive to change of specific parameters, then the inverse problem can be effectively solved. Though, parameters which do not have any effect on model response in a sensible manner are not simply identifiable, therefore should be put aside from the estimation procedure (Gallina *et al*. 2017). The efficiency of an optimization problem can be enhanced by reducing number of unknown parameters using Sensitivity Analysis (SA). If the sensitivities of some unknown parameters are much lower than others, then the performance of the identification process for those specific parameters is not reliable, i.e., the error in the reconstructed parameters is high (Vishnuvardhan *et al*. 2007b). For these reasons, it is very useful to run a sensitivity analysis before the identification process be carried out.

2.2.1 Base structure parameters

According to selected model to simulate wave propagation in the base structure and the configuration of piezoelectric transducers attached to the plate, three parameters of the plate affect the response: Young's modulus, mass density and Poisson ratio. These quantities are present in the Eqs. (1)-(2) through Lame constants and eventually through pressure (c_p) and shear (c_s) wave speeds. Because Young's modulus, density and Poisson ratio are not independent and are linked together via these two wave speeds, only two of these parameters could be identified independently. Since density is simple to measure directly relative to other parameters, it is considered as known and two other parameters are left to be identified. According to Eq. (5), Young's modulus and Poisson ratio are inserted into Eqs. (1)-(2) via pressure and shear wave speeds. Thus, for the rest of paper unknown parameters, Young's modulus and Poisson ratio are replaced with pressure and shear wave speeds for brevity. After identification of wave speeds, Young's modulus and Poisson ratio are calculated readily based on last two relations of Eq. (5) as

$$E = \rho c_S^2 \frac{3(c_P/c_S)^2 - 4}{(c_P/c_S)^2 - 1}, \qquad \nu = \frac{(c_P/c_S)^2 - 2}{2((c_P/c_S)^2 - 1)} \tag{9}$$

2.2.2 Piezoelectric material parameters

Thickness, length and width (for rectangular patch), Young's modulus, Poisson ratio, piezoelectric charge

Table 1 Parameters used in sensitivity analysis and their bounds

	Definition	min	max	
c_p	Pressure wave speed	5700	6300	(m/s)
c_s	Shear wave speed	2900	3300	(m/s)
ρ	Mass density of plate	2000	9000	(kg/m^3)
h	Thickness of plate[1]	0.4	5	$\times 10^{-3}$ (m)
s	Actuator to sensor distance	90	250	$\times 10^{-3}$ (m)
a	Half-length of piezoelectric[2]	1.5	5	$\times 10^{-3}$ (m)

[1]$h = 2d$; [2]length and width of piezoelectric patches are considered to be equal for both actuator and sensor

Table 2 PCE-based sensitivity analysis and resulted Sobol indices

	Sobol index	Value	Total Sobol index	Value
c_p	S_1	0.00039	S_1^T	0.05600
c_s	S_2	0.00036	S_2^T	0.05676
ρ	S_3	0.00002	S_3^T	0.05646
h	S_4	0.00753	S_4^T	0.15420
s	S_5	0.00056	S_5^T	0.06343
a	S_6	0.80479	S_6^T	0.94779

constant d_{31}, piezoelectric voltage constant g_{31} are piezoelectric material parameters incorporated in the model. Among parameters regarding piezoelectric transducer, length and width are quantities that could vary case wise since piezoelectric patches are usually cut to size manually according to each structure requirement, hence their dimension might come with large error. Thus, length and width of piezoelectric patch are also considered as unknown quantities to be identified. Other parameters have no influence on shape of response according to Eqs. (1)-(2), and they just have a scaling effect on the response i.e., only alter its magnitude. Therefore, their effects can efficiently be factored out by normalization.

2.2.3 Geometrical parameters

Two geometrical dimensions are also of great importance affecting response signal substantially: Relative position of sensor to actuator (x_c, y_c) on the plate and half the thickness of the plate (d). These two parameters are added to aforementioned unknown quantities summing up to five unknowns which are left to be identified.

2.3 Sensitivity analysis

As described in previous sections, efficiency of parameter identification can be significantly increased by preliminary sensitivity analysis. Sensitivity analysis in probabilistic modeling plays an important role in quantifying how uncertainty in the output of mathematical model is related to different sources of uncertainty in the input random variables. So, SA gives the information of which variables have the most and least effect on the output (response) of model. This is very useful especially where dimensionality of model inputs or parameters is high or forward solution is time consuming. Therefore, reduction of problem complexity is required. Methods of SA are usually classified into two categories: local and global sensitivity analysis. Local sensitivity analysis uses gradient of the response with respect to its parameters to assess the sensitivity of a model to those parameters. However, global sensitivity analysis measures the contribution of each parameter to the total variance over the entire domain, hence outcome of global SA is valid on whole space which parameters are defined in (Alexanderian 2013).

This paper uses Sobol index as a variance-based SA method. Monte Carlo simulation (MCS) is one of the conventional methods to calculate Sobol indices since it is straightforward and very simple to implement. Also, it is non-intrusive meaning it does not require to modify mathematical model (Shao *et al*. 2017). To further minimize computational costs, Polynomial Chaos Expansion (PCE) is employed as a meta-modeling (surrogate model) technique based on work done by Sudret (2008). According to mathematical model used to simulate wave propagation and section 2.2, different parameters used in SA are described in Table 1.

To perform the sensitivity analysis, the bounds on subjected parameters should be defined. These limits are also presented in Table 1. Since isotropic metallic materials are considered, bounds on pressure/shear wave speeds are assumed in such a way that most of common metals are included. The other physical property of plate material is mass density. In order to include most common metals, lower and upper limits for this parameter are considered from 2000 to 9000 kg/m^3. For thickness of base structure, bound is defined from 0.4 to 5 mm in order to assure generation of Lamb waves in the plate. Based on model used to simulate propagated waves, only incident waves from actuator to sensor are considered and reflected waves from boundaries are not modeled. Therefore, actuator and sensor positions relative to each other and boundaries should be set in a way that no boundary reflected waves interfere with incident waves. According to this, minimum distance of actuator-sensor distance is set to 0.09 m (no interference of modes) and maximum distance is set to 0.25 m (limited by size of plates in experiments). Dimension of piezoelectric patch is limited by experimental set-up. In this study, length and width of patches are considered to be equal and from 3 to 10 mm where their half-length is reported in Table 1. Considering quantities in Table 1 and their bounds, PCE-based sensitivity analysis is performed and results are reported in Table 2.

Based on SA result in Table 2, most influential quantities on response are dimension of transducers, thickness of base structure, actuator to sensor distance, pressure wave speed and shear wave speed in descending order, respectively. Though main goal is to estimate base structure characteristic parameters such as pressure and shear wave speeds and thickness, identification of geometrical quantities such as dimension of piezoelectric patch, and actuator to sensor distance is inevitable due to their higher influence on the response. Eventually, to gain

higher accuracy in determining Young's modulus of base structure, all parameters reported in Table 2 except mass density which is assumed to be known, have to be considered in parameter estimation process.

2.4 Inverse problem: Bayesian approach

The main idea behind Bayesian approach is to relate prior belief on the errors and unknowns to prior probability laws, using these laws and combine them with measurement data to infer unknowns or posterior probabilities. The chief benefit of the Bayesian inference is that it treats the unknowns, denoted by the vector θ, as random variables with joint distribution $p(\theta)$. Two main sources of noise are usually measurement and model error (Reed *et al*. 2018). However, a validation study on the mathematical model is conducted which shows selected model could effectively capture wave propagation dynamic such that the total noise term in the problem is dominated by measurement noise and not model error. In this perspective, assume N-point structure response z_n and noise-free response y_n. The difference of two later variables is a sequence of independent and identically distributed (i.i.d) Gaussian variable with zero mean and unknown variance σ_G^2 (Jaynes 2003). Thus, likelihood distribution can be written as

$$p_L(z|\theta,\sigma_G^2) = \frac{1}{(2\pi\sigma_G^2)^{N/2}} exp\left[-\frac{1}{2\sigma_G^2}\sum_{n=1}^{N}\left(z_n - y_n(\theta)\right)^2\right] \quad (10)$$

By this definition, dependence of likelihood function on the unknown vector θ is specified by model response $y_n(\theta)$. The likelihood is a probabilistic statement about the distribution of observed data z_n given a model response, determined by parameter vector θ. For convenience, parameter vector henceforth includes noise variance. Two important assumptions are made at this stage. First, measurement noise is uncorrelated. Second, structure response obtained at different locations has the same variance denoted by σ_G^2. Neither assumptions are mandatory since noise variance for each measurement could be estimated separately. Based on Bayes theorem, prior parameter Probability Density Function (PDF), $p_\pi(\theta)$ is related to the posterior $p(\theta|z)$ via likelihood function as

$$p(\theta|z) = \frac{p_L(z|\theta)p_\pi(\theta)}{p_D(z)} \quad (11)$$

The term in the denominator is usually ignored since it's a normalizing constant. To calculate probability distribution of each unknown, one has to obtain marginal distribution for that unknown based on joint parameter distribution

$$\begin{aligned} p(\theta_j|z) &= \int_{\mathbb{R}^{P-1}} p(\theta|z)d\theta_{-j} \\ &\propto \int_{\mathbb{R}^{P-1}} p_L(z|\theta)p_\pi(\theta)d\theta_{-j} \end{aligned} \quad (12)$$

where $\int_{\mathbb{R}^{P-1}} d\theta_{-j}$ denotes integral over all parameters other than θ_j. Thus, a high dimensional integral is required to be calculated involving a likelihood function with usually complicated expression (Zhou *et al*. 2015). Fortunately, in this case, there is convenient numerical approaches sampling from marginal parameter distributions instead of calculating the involved joint integral.

2.5 Markov-chain Monte-Carlo (MCMC) sampling

Instead of performing the integration on joint parameter distribution in Eq. (12) which is usually complex or time consuming, one can make use of Markov chain Monte Carlo method to sample directly from marginal distribution of unknown parameters. The key property of MCMC is that the generated Markov chains have stationary distributions equal to the desired marginal distributions. There are several algorithms to implement MCMC method. One particular MCMC method is the Gibbs sampler which is applicable to a broad class of Bayesian problems. The key to the Gibbs sampler is that it only considers univariate conditional distributions i.e., all of the random variables but one, are assigned fixed values. Such conditional distributions are easier to simulate than complex joint distributions and usually have simple forms such as normal, inverse Chi squared, or other common prior distributions. Thus, *n* random variables are simulated sequentially from the *n* univariate conditionals rather than generating a single *n*-dimensional vector using the full joint distribution. Consider a parameter vector $\theta = (\theta_1, \theta_2, \dots, \theta_P)'$, data z, prior $p_\pi(\theta)$, and likelihood $p_L(z|\theta)$. Here vector θ_{-j} is defined as the parameter vector by deleting the *j*th component. Gibbs sampling of the posterior distribution of Eq. (11) generates a Markov chain $\{\theta^{(i)}\}, i = 1$ to chain-length wherein components of vector $\theta_j^{(i)}$ generated sequentially for $j = 1, 2, \dots, P$. Vector component $\theta_j^{(i)}$ is sampled from its full conditional distribution $p\left(\theta_j^{(i)}|z, \theta_{-j} = \theta_{-j}^{(i-1)}\right)$. The full conditional distribution of θ_j is like posterior distribution of θ_j, assuming other P-1 parameters were known and equal to their value of last chain: $\theta_k = \theta_k^{(i-1)}$ for $k \neq j$. Thus, similar to posterior distribution of Eq. (11) full conditional distribution is proportional to product of likelihood and prior

$$p\left(\theta_j^{(i)}|z, \theta_{-j} = \theta_{-j}^{(i-1)}\right) = p_L(z|\theta)p_\pi(\theta) \quad (13)$$

To obtain probability distribution for each parameter using Gibbs sampling, one should only sample full conditional distribution of that parameter. If likelihood function and prior be from same parametric family, the resultant full conditional is from the same family as well. This provoke concept of conditional conjugacy. In this study error variance is sampled directly using conditional conjugacy and other unknowns are sampled using Metropolis-Hastings algorithm.

2.5.1 Sampling σ_G^2 by conditional conjugacy concept

Recalling error model of Eq. (10) with reparametrized factor $\tau = 1/\sigma_G^2$ known as precision parameter and

Goal: generating posterior distributions $p(\theta_j)$ in presence of model data y_n, observed data z_n and prior distributions $p_{\pi_j}(\theta_j)$ and estimating noise variance $\theta_{P+1} = \sigma_G^2$

Initialization: chain starts with $i = 0$

- Initial guess for parameter values (from prior distributions) $\boldsymbol{\theta}(0) = \theta_j(0)\ j = 1, \dots, P$
- Sampling prior variance from inverse gamma distribution $\theta_{P+1}(0) = \mathrm{IG}(N/2 + 1, \left(\sum_{n=1}^{N}(z_n - y_n(\theta_0))^2\right)/2)$
- B is number of burn-in samples

Main loop: increase i by 1 and
for each j

- Generate candidate $\theta_j^* = \theta_j(i-1) + 2A_j \times U(-1,1)$ with A_j as half-length of θ_j range and $U(-1,1)$ is uniform distribution from -1 to +1
- Calculate ratio R as stated in text
  - If $U(0,1) < R$ candidate value is accepted e.g. $\theta_j(i) = \theta_j^*$
  - otherwise candidate value is rejected e.g. $\theta_j(i) = \theta_j(i-1)$

Variance posterior distribution is sampled directly $\theta_{P+1}(i) = \mathrm{IG}(N/2 + 1, \left(\sum_{n=1}^{N}(z_n - y_n(\theta_i))^2\right)/2)$
After $i > B$ iterations values for $\theta_j(i)$ are stored as members of $p(\theta_j)$

Fig. 3 Algorithm of parameter estimation presented as pseudocode

assuming independent priors for $p_\pi(\tau)$ and $p_\pi(\theta)$, full conditional distribution can be written as

$$p(\theta, \tau|z) \propto \tau^{N/2}\, exp\left(-\frac{\tau}{2}\sum_{n=1}^{N}\left(z_n - y_n(\theta)\right)^2\right) p_\pi(\tau) p_\pi(\theta) \quad (14)$$

therefore, the full conditional distribution for τ is

$$p(\tau|z, \theta) \propto \tau^{N/2}\, exp\left(-\frac{\tau}{2}\sum_{n=1}^{N}\left(z_n - y_n(\theta)\right)^2\right) p_\pi(\tau) \quad (15)$$

In Eq. (15) the unknown vector prior $p_\pi(\theta)$ has been dropped as it is simply a proportionality constant with respect to τ. Recalling gamma distribution with general density function of the form $p(x) \propto x^{\alpha-1}exp(-\beta x)$ for $x > 0$ and parameters $\alpha, \beta > 0$, thus likelihood function in Eq. (15) is a distribution from gamma family. Moreover, if one chooses a gamma prior for τ with parameters α and β, the full conditional distribution is also in the gamma family with parameters $\alpha' = \alpha + N/2$ and $\beta' = \beta + \left(\sum_{n=1}^{N}\left(z_n - y_n(\theta)\right)^2\right)/2$. Thus, one could directly sample τ (hence σ_G^2) from Inverse Gamma (IG) distribution which has a simple relation with gamma (G) distribution: $IG(a,b) = 1/G(a, 1/(a,b))$. Implementing uninformative prior, obtained by setting $\alpha = 1$, $\beta = 0$ and P unknowns excluding variance, variance in ith link of Markov chain is sampled from

$$\theta_{P+1}(i) = \frac{1}{G\left(\frac{N}{2} + 1, \frac{2}{\sum_{n=1}^{N}(z_n - y_n(\theta_i))^2}\right)} \quad (16)$$

2.5.2 Sampling θ using Metropolis-Hastings algorithm

Despite of variance, conjugate or conditionally conjugate prior is not available for unknown vector θ. In this situation where sampling of full conditional distribution (Eq. (12)) is required, Metropolis–Hastings algorithm is one of several techniques known as rejection sampling giving simplicity and generality to sample the full conditional distribution with no special assumptions. Since conditional distribution for parameter τ was sampled directly, left hand side of Eq. (12) can be demonstrated by $f(\theta)$ where $f(\theta) = p(\theta_j)$. The Metropolis-Hastings algorithm generates a sequence $\{\theta^{(i)}\}$ based on following procedure (Nichols *et al*. 2010):

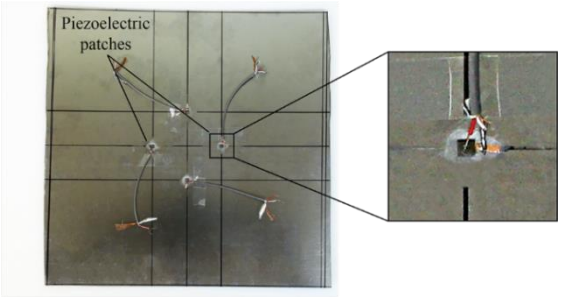

Fig. 4 Fabricated specimen as experimental set-up with piezoelectric transducers (PZT-5H)

• A candidate parameter θ^* is drawn from a proposal density $g(x|\theta^{(i-1)})$ based on current value $\theta^{(i-1)}$.

• The ratio $R = \frac{f(\theta^*) \times g(\theta^{(i-1)}|\theta^*)}{f(\theta^{(i-1)}) \times g(\theta^*|\theta^{(i-1)})}$ is computed.

• A Bernoulli trial is performed with probability $R' = \min\{R, 1\}$.

• If success, $\theta^i = \theta^*$, otherwise, $\theta^i = \theta^{(i-1)}$.

• $i = i + 1$ is set and again from step 1 other draws are obtained.

According to MCMC theory, distribution to which the resultant Markov chain converges, will be the desired posterior distribution, regardless of the starting values chosen for unknown parameters. Although, poor starting values (far from high probable regions of stationary distribution) may cause the algorithm to reject many candidates and leading to long run times (Lynch 2007). Moreover, implementation of MCMC algorithm is linked to the desired distribution only by the ratio R. Thus, in calculating R, the normalizing constants in the denominator of Eq. (11) which makes the distribution integrate to 1, would be canceled out. Therefore, the denominator which is an enormous concern in calculating full conditional distributions, does not need to be calculated (Nichols *et al*. 2010). Fig. 3 provides algorithm of parameter estimation process and steps.

Table 3 Physical specification of test plates

Material	Grade	L (mm)	h (mm)	E (GPa)	ρ (kg/m^3)	ν (mm/mm)
Steel	CK75	30	0.5	210	7860	0.30
Steel	CK75	40	1.0	205	7850	0.30
Steel	CK75	40	1.5	205	7850	0.30
Steel	ST304	40	0.8	193	8000	0.29
Aluminum	1100	40	0.5	69	2700	0.33
Aluminum	1100	40	0.8	69	2700	0.33
Aluminum	1100	40	1.0	69	2700	0.33

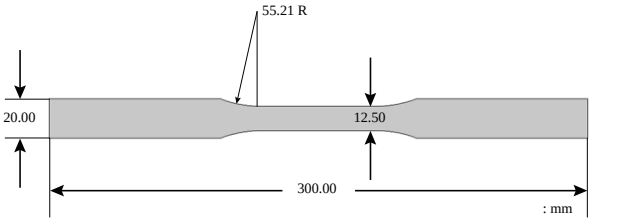

(a) Schematic with dimensions

(b) Water jet-cut specimen

Fig. 5 Standard specimen for measuring Young's modulus using tensile test according to ASTM E8

3. Experiments

Experimental tests and measurements are a critical part of every parameter estimation experience. One should carefully select quantities to be measured. This step significantly reduces experiment complexity and errors originated from obtained data (Pagnotta 2008, Araujo *et al*. 2009). From this point of view, the question of what should be considered as structure response, arises. Practically, response of structure should have several features:

• It should be simple to be measured.

• The sensor should preferably be simple and cheap.

• Response should contain as much structure features as possible. i.e., variation of unknown parameters has a strong effect on response (response enrichment).

• The response can be collected without inference with performance of structure in order to carry out parameter estimation (in-situ implementation of method).

In the present paper, impulse excitation is selected since structure response to this excitation fulfills above criteria. Analytical solution presented in section 2.1 which experimental results are compared with, considers infinite plates only, thus reflected waves from boundaries are not included in the response. As impulse excitation generates multimodal and mixed Lamb waves in thin plates, it is easy to remove reflections from response using Time Of Flight (TOF). Two fundamental symmetric and antisymmetric modes of Lamb wave (S_0 and A_0) are taken into account in this study, however there is no restriction to consider higher modes.

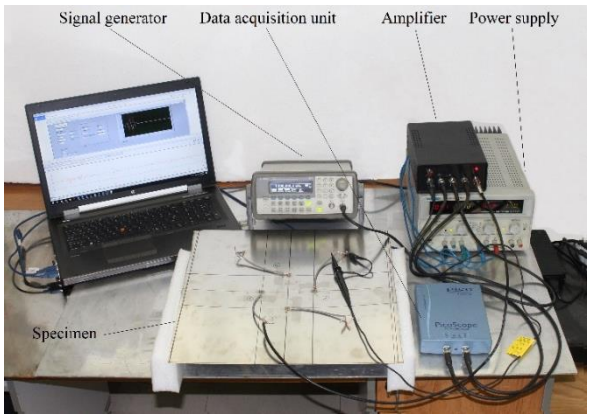

Fig. 6 Experimental set-up for exciting the structure and measuring the response of plate specimens

3.1 Test structures

For experimental tests two materials, steel and aluminum are selected due to their widespread industrial applications. Seven square plates are cut from these materials. Two identical piezoelectric patches (PZT-5H) as actuator and sensor are bonded to each plate. Distance between actuator and sensor and distance between each of them to plate boundaries are set such that reflected waves from boundaries wouldn't affect two fundamental modes of incident Lamb wave (more details are given in section 3.3). This way, one can separate response of the plate to only contain S_0 and A_0 modes. Fig. 4 shows base plate equipped with two piezoelectric patches as actuator and sensor for which unknown parameters are required to be determined.

Geometrical and mechanical properties of base plates are demonstrated in Table 3. In this study, however actuator to sensor distance and half-length of piezoelectric patches (s and a) are not objective, but in order to show performance of the proposed method while number of unknowns increases, these parameters are taken into account and kept constant in parameter estimation process. Their values are equal to s = 100 mm and a = 2.5 mm for the sake of experiments. Quantities reported in Table 3 are based on direct measurement or material datasheets. For example, Young's modulus is measured based on ASTM E8 standard for tension testing of metallic materials. For this test, standard specimen (Fig. 5) are cut out of same sheets (Table 3) and geometrical dimensions are measured directly. Standard specimens are water jet-cut to reduce heat induced alteration in material structure.

3.2 Experimental setup

Experimental set-up to excite plates and record their response is shown in Fig. 6. A signal generator (AWG 33220A by Agilent) and an amplifier is used to apply the excitation signal to actuator transducer and an oscilloscope (PicoScope 4424 by Pico Technology) is used to capture structure response through the sensor. Repeated response signals are recorded and averaged to improve signal to noise ratio.

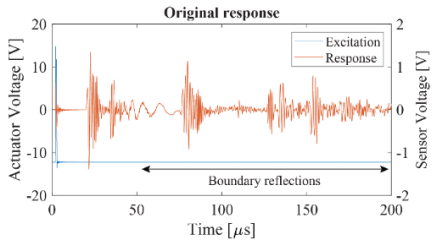

(a) Original temporal excitation and resulted response with boundary reflections

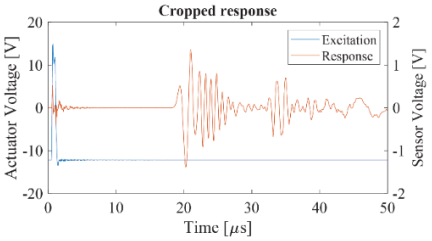

(b) Cropped temporal signals

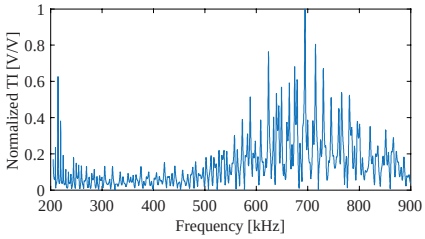

(c) Normalized TI based on original temporal signals

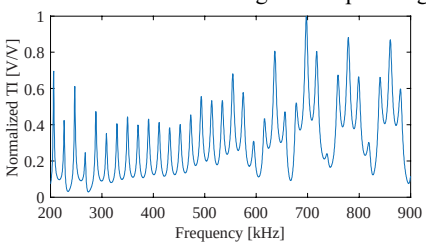

(d) Normalized TI based on cropped temporal signals

Fig. 7 Recorded response from the steel plate (h = 1 mm, E = 200 GPa, ρ = 7850 kg/m^3, ν = 0.3) by experimental tests

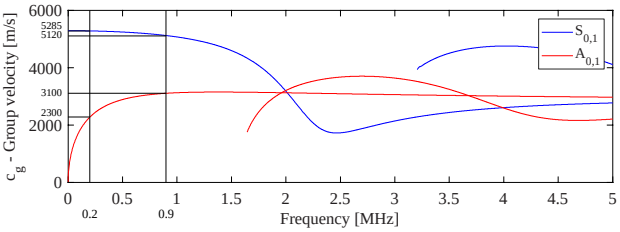

Fig. 8 Group velocity dispersion curves for two first symmetric and antisymmetric modes of Lamb waves for a steel plate with $h = 1$ mm, $E = 200$ GPa, $\rho = 7850$ kg/m^3 and $\nu = 0.3$

3.3 Excitation signal and boundary reflections removal

To excite plates and record their response, a novel efficient method developed experimentally by same authors (Asadi *et al*. 2017) is implemented. In this method an impulse signal is applied to the actuator patch exciting the structure in a wide frequency range (Fig. 7(a)). Generally, in Lamb wave-based studies, excitation signal is selected in a way that a frequency range with narrow band is excited to minimize dispersion effect exists with guided waves in plates. However, response recorded based on a narrow band excitation (tone burst), contains much less information about structure properties comparing to a wide band excitation. A rich response ultimately leads to better estimation of unknown parameters. The resulted response due to an impulse excitation is generally a multi-mode, multi-frequency Lamb wave since a wide range of frequencies is excited by impulse excitation. Signal processing is done in two time and frequency domains separately. In time domain, one should window response in order to remove boundary reflections in the experiments.

Since Dispersion Curves (DC) for steel and aluminum do not change dramatically, it can be done using a generic dispersion curve with approximate values for properties of the base plate. Fig. 8 shows group velocities for first two symmetric and antisymmetric modes of Lamb waves for a steel plate with h = 1 mm, E = 200 GPa, ρ = 7850 kg/m^3 and ν = 0.3. For frequency range of interest (200 to 900 kHz), velocity variation of Lamb modes is determined and their corresponding reception time is calculated according to the distance between actuator and sensor. For 200 to 900 kHz, velocity of two fundamental Lamb wave modes varies between 5285 to 5120 m/s for S_0 mode and 2300 to 3100 m/s for A_0 mode, respectively. Thus, arrived waves are expected in the time window of 18.9 to 19.5 μs for S_0 and 32.2 to 43.5 μs for A_0 according to actuator-sensor distance (100 mm). Therefore, for this setup, any received wave after 43.5 μs (corresponding to the wave with lowest velocity, A_0 at 200 kHz) is contributed to the reflections from boundaries or higher modes. This is worthy to mention that, this is only an estimation for a typical plate, to consider variation in material properties, some larger time window should be selected. Any wave arriving after 50 μs can be considered as boundary reflection or higher mode, hence is discarded (Fig. 7(b)). This time window is fixed and applied on every experimental data sets for different materials. Then, frequency domain operation is carried out in order to calculate transfer impedance for wave propagation path.

After cropping original temporal signal in order to remove boundary reflections, time domain signals of excitation and response are transformed into frequency domain using Fast Fourier Transform (FFT). Fourier transform of response is divided by Fourier transform of excitation signal to give transfer function of wave path or Transfer Impedance (TI) (Bhalla *et al*. 2009). Figs. 7(c)-(d) show TI before and after removing boundary reflections. It should be noted that the better process of removing boundary reflections is performed, more accurate the estimation will be. Though this is for a typical steel plate, proposed applied procedure can be a primordial step for the unknown parameter estimation process. After obtaining experimental transfer impedance, same procedure is repeated with analytical response generated by Eq. (7).

Table 4 Prior bounds of unknown parameters for initializing Gibbs sampler

Parameter	Lower bound	Upper bound	
c_p	5700	6300	(m/s)
c_s	2900	3300	(m/s)
h	0.4	2	$\times 10^{-3}$ (m)
s	95	110	$\times 10^{-3}$ (m)
a	1	3	$\times 10^{-3}$ (m)

It is worth to mention that in analytical solution amplitude of excitation is assumed to be unity at all frequencies. This assumption is not applicable in experimental tests due to non-ideal equipment so the excitation amplitude has different values at different frequencies. This difference in analytical and experimental TIs can be compensated by dividing transformed analytical response by transformed experimental excitation instead of analytical excitation which has fixed amplitude equal to 1. This means analytical response is generated when exactly experimental excitation is applied to the mathematical model. According to Eq. (10), in this study model response y_n is the analytical transfer impedance and z_n is the transfer impedance obtained by experiments. Thus, dependency of likelihood PDF to unknown parameters is through model response y_n which is function of those parameters.

4. Results and discussion

For each structure in Table 3, Bayesian inference is carried out to estimate unknown parameters by implementing Gibbs sampling. The Gibbs sampling which is a member of general class of MCMC algorithms, provides an approximation of the entire posterior PDF, regardless of its underlying form. For initial state of chains, each parameter range is divided into four equal length sections with four points as their lower boundary since computations are conducted on a CPU with four cores. Each of these points are initial values for four parallel Markov chains. By completion of the process, these parallel chains are combined together to make one bigger chain for each parameter. This method eliminates any biasing that might be result of initialization. Moreover, it creates a framework which makes parallel processing readily available by adding more CPUs or cores. This capability significantly reduces run time for each chain to converge. Table 4 demonstrates unknown parameters bounds. Uniform distribution (non-informative) over each parameter range is assumed. Spans for pressure and shear speeds are considered such a way that most steel and aluminum alloys can be taken into account. Also, span for thickness parameter includes thickness of all specimens where used in the experimental tests. Values for s and a are researcher's choice and can be selected according to experimental conditions.

Generally, it is not possible to determine number of iterations required for convergence of Markov chain in advance. The convergence is typically evaluated using variance-based methods (Reed *et al.* 2018). In this study, convergence is monitored sequentially, as the chains evolve. Every 10000, 25000, 50000 and 100000 iterations, PDFs for chains are evaluated, if PDFs remain almost unchanged

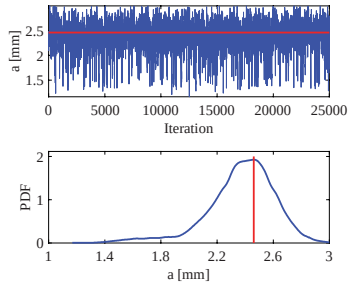

(a) Half-length of piezoelectric transducer

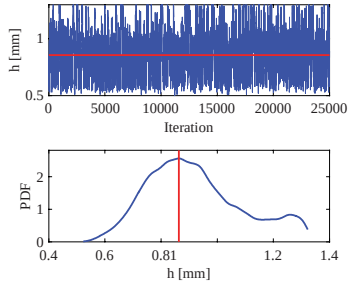

(b) Thickness of the base plate

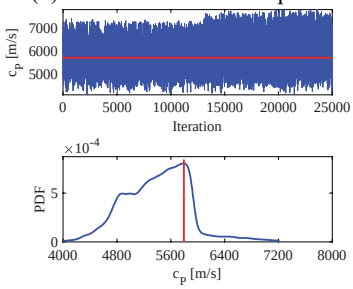

(c) Speed of pressure wave

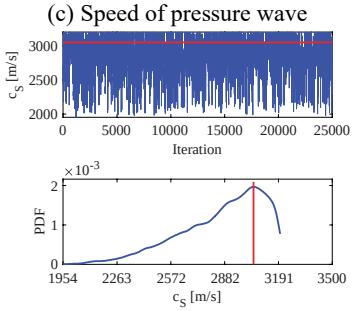

(d) Speed of shear wave

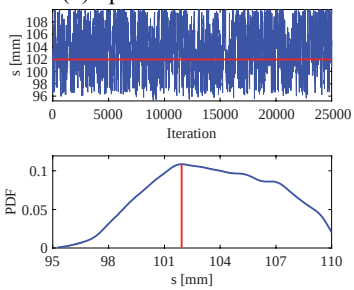

(e) Distance between sensor and actuator

Fig. 9 Trace histories for unknown parameters and their corresponding estimated PDFs for plate #4. For each trace and PDF their mode statistic is presented with a red line

Table 5 Estimated mean value for speed of pressure wave against length of Markov chains

	Number of iterations	Mean (m/s)	CV (%)
1	10000	5942	10
2	25000	5749	9
3	50000	5632	8
4	100000	5612	8

relative to last sequence, then one could interpret that chains have reached their stationary state. In all Markov chains, first 10 percent of samples are discarded as burn-in and remaining samples are assumed to be sampled from posterior marginal distribution of unknown parameters.

Fig. 9 shows traces of Markov chains generating parameters in the upper section and histogram of trace histories in the lower section for five unknown parameters. Test specimen used to obtain data of Fig. 9 is 0.8 mm thick ST304 stainless steel plate (plate #4 in Table 3). It is evident that trace histories for unknown parameters do not converge to specific values. This indicates that many combinations of unknown parameters may result a similar structure response and these combinations are equally as likely. Moreover, the chains appear to mix well indicating parameter spans are scanned quite well by Markov chains for all parameters. Since trace histories obtained by MCMC method are not supposed to verge toward a single solution, one can monitor convergence of Markov chains by variance-based methods. Since probability distributions for parameters are not strictly symmetric, normal distributions are not adequate to represent them. In this study, the following procedure is proposed to determine estimations about unknowns.

Histogram of trace histories are calculated. Then Kernel Density Estimation (KDE) is applied to fit kernel-smoothing distributions on the parameter histograms. Resulted PDFs represent probability distributions for parameters more conveniently, since KDE smooths out some irregularities which may appear in histograms obtained from trace histories. To locate regions of high density, one can use any mode-finding method. The mode statistic is less influenced by the irregularities in estimated PDFs and tails of the data. In this study, simply the maximum of kernel estimated PDFs is considered as target values representing marginal posterior distribution of unknown parameters.

Carrying out above procedure for different number of iterations provides an estimation about required iterations for Markov chains to converge. Table 5 shows mean statistic and it's Coefficient of Variation (CV) for estimated speed of pressure wave for specimen #4, against four different length of Markov chains. It is noted that with increasing number of iterations, CV which is a measure for dispersion of probability distribution decreases. Iterations higher than 25000 does not result to any significant reduction in CV. Same results are observed with Markov chains for other parameters and other specimens. Therefore, further investigations are based on 25000 iterations.

For all specimens presented in Table 3, proposed procedure is applied and resulted marginal posterior distributions for unknown parameters are obtained. Then, estimation is made based on mode statistic. In Table 6, resulted identified parameters are compared with actual values obtained by standard tests or direct measurements. For estimated parameters, coefficient of variation and their error relative to true values is provided.

Table 6 Estimated unknowns for different steel and aluminum plates compared to true values

	Specimen		Estimated value	CV %	True value	|Error| %
#1	Steel CK75	c_p	6256	3	5997	4
		c_s	3123	2	3206	3
		h	0.56	6	0.50	12
		s	107	3	100	7
		a	2.40	7	2.50	4
#2	Steel CK75	c_p	5789	4	5929	2
		c_s	3184	3	3169	1
		h	0.88	6	1.00	12
		s	101	3	100	1
		a	2.14	16	2.50	14
#3	Steel CK75	c_p	6237	3	5929	5
		c_s	3128	3	3169	1
		h	1.27	7	1.50	15
		s	102	3	100	2
		a	2.11	9	2.50	15
#4	Steel ST304	c_p	5749	9	5623	2
		c_s	3037	8	3058	1
		h	0.87	4	0.80	9
		s	102	3	100	2
		a	2.46	10	2.50	2
#5	Aluminum 1100	c_p	5742	3	6153	7
		c_s	3118	2	3099	1
		h	0.58	8	0.50	16
		s	106	3	100	6
		a	2.87	5	2.50	15
#6	Aluminum 1100	c_p	5830	4	6153	5
		c_s	2949	3	3099	5
		h	0.82	15	0.80	3
		s	107	3	100	7
		a	2.71	5	2.50	8
#7	Aluminum 1100	c_p	6236	3	6153	1
		c_s	3128	3	3099	1
		h	1.17	15	1.00	17
		s	102	3	100	2
		a	2.11	9	2.50	15

Table 6 shows results for each estimated parameters considering maximum error for estimated values. Maximum error in estimated pressure, shear wave speeds and thickness of base structure is 7%, 5% and 17%,

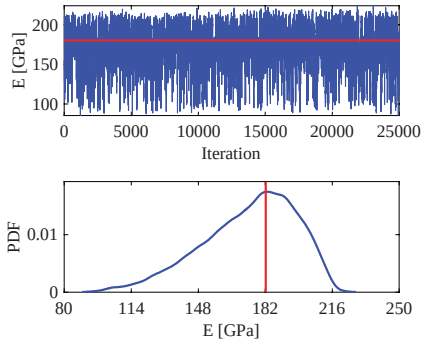

(a) Young's modulus

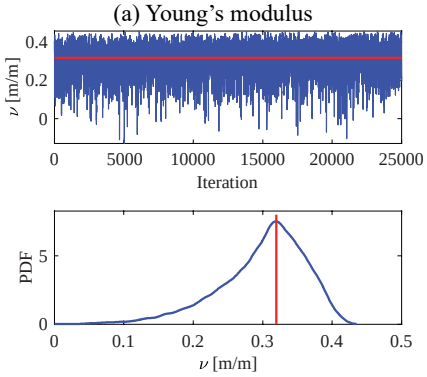

(b) Poisson ratio

Fig. 10 Trace histories for Young's modulus and Poisson ratio chains calculated according to Eq. (9) and their corresponding estimated PDFs for plate #4. Mode statistic is presented with a red line

Table 7 Estimated Young's modulus and Poisson ratio for plates of Table 4 compared with true values

	Specimen		Estimated value	CV %	True value	|Error| %
#1	Steel CK75	E	201	4	210	4
		ν	0.322	6	0.30	7
#2	Steel CK75	E	204	4	205	1
		ν	0.326	8	0.30	9
#3	Steel CK75	E	202	4	205	2
		ν	0.326	6	0.30	9
#4	Steel ST304	E	182	14	193	6
		ν	0.321	22	0.29	11
#5	Aluminum 1100	E	69.2	4	69	0
		ν	0.324	6	0.33	2
#6	Aluminum 1100	E	63.5	4	69	8
		ν	0.328	6	0.33	1
#7	Aluminum 1100	E	70	4	69	1
		ν	0.323	6	0.33	2

respectively. This acceptable accuracy in estimation of material properties indicates capability of proposed method, regarding its in-situ and nondestructive nature. Also, maximum error for two other parameters are 7% and 15% for s and a. Since changing material does not change solution time, all simulations need an equal time to be completed. Hence, each iteration in which all five parameters are estimated simultaneously, needs about 0.28 second to be solved, so for each Markov chain containing 25000 iterations, solution time is equal to 116 minutes.

One can obtain Young's modulus of material based on pressure and shear wave speeds, given mass density as it was notified in Eq. (9). Fig. 10 shows estimated values for Young's modulus and Poisson ratio for plate #4 based on data reported in Fig. 9 using Eq. (9). As it was reported before, trace histories show well-mixed chains which are not converged to single solutions. Kernel-smoothed PDFs are presented in the lower section of Fig. 10 segments and their modes are specified. Estimated Young's modulus and Poisson ratio for other specimens are reported in Table 7 and compared with true values. It is evident that estimated values for Young's modulus and Poisson ratio which were the main objective of this paper are determined with significant accuracy for seven different steel and aluminum plates. Maximum error in the estimation process is below 8% for E and 11% for ν. Among previous works incorporating Bayesian method, Reed *et al.* (2018) proposed a model based Bayesian characterization of material for a composite plate using contact transducer to generate guided waves and a laser Doppler vibrometer to collect out of plane velocity signal. They achieved error of 7%, 1%, 17% and 24% in estimation of E_{11}, $E_{22}(E_{33})$, $G_{12}(G_{13})$ and ρ, respectively.

Gallina *et al.* (2017) introduce a dispersion curve-based Bayesian estimation for composite plates with a piezoelectric actuator and laser vibrometer as sensor. They reached error equal to 1, 2, 1 and 27 percent for estimation of E_1 (in-line with fiber), E_2 (perpendicular to fiber), G_1 and ρ. Considering that proposed method in this paper is solely based on electrical signals received from piezoelectric transducers and it not using any complicated device to measure dynamic parameters such as displacement or velocity, achieved accuracy in estimation of elastic parameters is comparable with works that used such devices.

It is worthy to mention that however geometrical and mechanical parameters are introduced in Table 7 as true values, but these values are accompanied with experimental errors. The advantages of the proposed method are discussed as below:

• Methodology presented in this study gives researchers a great ability to take various unknowns into account based on used mathematical model.

• Main limitation of the procedure seems to be connected with the modeling step since only simple structures can be identified. To overcome this limitation, proposed method can be modified by replacing analytical model with other type of models such as finite element model for more complex geometries which are more applicable in industrial purposes.

• By implementing proposed method there is no need to remove specimen from original structure. Moreover, access to only one side of structure is enough to probe ultrasonic guided wave propagation. Also, the only experimental data it uses is the structure response to an excitation where both

the excitation and response are measured via piezoelectric transducers. As only electrical signals are required to be measured, data acquisition equipment becomes much simpler contrary to other types of structure responses such as displacement or velocity which need rather more complicated equipment.

• This method is nondestructive. Additionally, it uses both symmetric and antisymmetric fundamental modes, i.e., there is no need to separate these two modes hence decreasing complexity of signal processing stage. The ability to simultaneously estimate transmitter and receiver characteristics as well as medium properties is another advantage of proposed procedure. Besides, it is wave-based instead of vibration-based which independents the parameter estimation problem from boundary conditions.

5. Conclusions

In the present paper, a new approach is proposed to estimate physical properties of plate-like structures non-destructively. Main targets of estimation are Young's modulus, Poisson ratio and thickness of different aluminum and steel plates. Moreover, along with these parameters, piezoelectric patch dimension and distance between actuator to sensor are also determined. The proposed approach uses Bayesian inference which is robust in condition of parameter, modeling and measurement uncertainty. To determine most effective parameters on structure response, a sensitivity analysis is performed using polynomial chaos expansion. Estimation of unknown parameters is carried out based on response signals resulted from impulse excitation of structure using piezoelectric actuator and sensor. A signal processing procedure is presented to remove boundary reflected waves from responses. Then experimental and simulated data are combined in a Bayesian framework for parameter identification. Sampling of posterior marginal distributions for estimated parameters is performed using Gibbs sampling. Young's modulus and Poisson ratio for test structures are estimated with maximum errors of 8 and 11 percent, respectively. Moreover, proposed non-destructive and in-situ method not only can estimate the mechanical and geometrical parameters but also can be integrated into present implemented structural health monitoring systems.

References

Ablitzer, F., Pézerat, C., Génevaux, J.M. and Bégué, J. (2014), "Identification of stiffness and damping properties of plates by using the local equation of motion", *J. Sound Vib.*, **333**(9), 2454-2468. https://doi.org/10.1016/j.jsv.2013.12.013.

Agrahari, J.K. and Kapuria, S. (2016), "A refined Lamb wave time-reversal method with enhanced sensitivity for damage detection in isotropic plates", *J. Intell. Mater. Syst. Struct.*, **27**(10), 1283-1305. https://doi.org/10.1177/1045389X15590269.

Akgöz, B. and Civalek, Ö. (2017), "Effects of thermal and shear deformation on vibration response of functionally graded thick composite microbeams", *Compos. Part B Eng.*, **129**, 77-87. https://doi.org/10.1016/j.compositesb.2017.07.024.

Alexanderian, A. (2013), "On spectral methods for variance based sensitivity analysis", *Probab. Surv.*, **10**, 51-68. https://doi.org/10.1214/13-PS219.

Ambrozinski, L., Packo, P., Pieczonka, L., Stepinski, T., Uhl, T. and Staszewski, W. (2015), "Identification of material properties–efficient modelling approach based on guided wave propagation and spatial multiple signal classification", *Struct. Control Health Monit.*, **22**(7), 969-983. https://doi.org/10.1002/stc.1728.

Arani, A.J. and Kolahchi, R. (2016), "Buckling analysis of embedded concrete columns armed with carbon nanotubes", *Comput. Concrete, Int. J.*, **17**(5), 567-578. https://doi.org/10.12989/cac.2016.17.5.567.

Araujo, A.L., Soares, C.M.M. and De Freitas, M.M. (1996), "Characterization of material parameters of composite plate specimens using optimization and experimental vibrational data", *Compos. Part B Eng.*, **27**(2), 185-191. https://doi.org/10.1016/1359-8368(95)00050-X.

Araujo, A.L., Soares, C.M.M., De Freitas, M.M., Pedersen, P. and Herskovits, J. (2000), "Combined numerical-experimental model for the identification of mechanical properties of laminated structures", *Compos. Struct.*, **50**(4), 363-372. https://doi.org/10.1016/S0263-8223(00)00113-6.

Araujo, A.L., Soares, C.M.M., Herskovits, J. and Pedersen, P. (2002), "Development of a finite element model for the identification of mechanical and piezoelectric properties through gradient optimisation and experimental vibration data", *Compos. Struct.*, **58**(3), 307-318.

Araujo, A., Mota Soares, C., Herskovits, J. and Pedersen, P. (2009), "Visco-piezo-elastic parameter estimation in laminated plate structures", *Inverse Probl. Sci. Eng.*, **17**(2), 145-157. https://doi.org/10.1080/17415970802082732.

Argyris, C., Chowdhury, S., Zabel, V. and Papadimitriou, C. (2018), "Bayesian optimal sensor placement for crack identification in structures using strain measurements", *Struct. Control Health Monit.*, **25**(5), e2137. https://doi.org/10.1002/stc.2137.

Asadi, S., Sepehry, N., Shamshirsaz, M. and Vaghasloo, Y. (2017), "Implementation of a novel efficient low cost method in structural health monitoring", *Smart Mater. Struct.*, **26**(5), 055032. https://doi.org/10.1088/1361-665X/aa6b65.

Attia, A., Tounsi, A., Bedia, E. and Mahmoud, S. (2015), "Free vibration analysis of functionally graded plates with temperature-dependent properties using various four variable refined plate theories", *Steel Compos. Struct., Int. J.*, **18**(1), 187-212. https://doi.org/10.12989/scs.2015.18.1.187.

Auzins, J. and Skukis, E. (2015), "Robust optimization approach for mixed numerical/experimental identification of elastic properties of orthotropic composite plates", *Proceedings of the VI International Conference on Computational Methods for Coupled Problems in Science and Engineering*, Venice, Italy, May.

Bales, B., Petzold, L., Goodlet, B.R., Lenthe, W.C. and Pollock, T.M. (2018), "Bayesian inference of elastic properties with resonant ultrasound spectroscopy", *J. Acous. Soc. Am.*, **143**(1), 71-83. https://doi.org/10.1121/1.5017840.

Banerjee, B. (2016), "Elastic parameter identification of plate structures using modal response: An ECE based approach", *J. Eng. Mech.*, **142**(1), 04015059. https://doi.org/10.1061/(ASCE)EM.1943-7889.0000970.

Battaglia, G., Di Matteo, A., Micale, G. and Pirrotta, A. (2018), "Vibration-based identification of mechanical properties of orthotropic arbitrarily shaped plates: Numerical and experimental assessment", *Compos. Part B Eng.*, **150**, 212-225. https://doi.org/10.1016/j.compositesb.2018.05.029.

Bhalla, S., Gupta, A., Bansal, S. and Garg, T. (2009), "Ultra low-cost adaptations of electro-mechanical impedance technique for structural health monitoring", *J. Intell. Mater. Syst. Struct.*,

20(8), 991-999. https://doi.org/10.1177/1045389X08100384.

Bochud, N., Laurent, J., Bruno, F., Royer, D. and Prada, C. (2018), "Towards real-time assessment of anisotropic plate properties using elastic guided waves", *J Acoust. Soc. Am.*, **143**(2), 1138-1147. https://doi.org/10.1121/1.5024353.

Civalek, Ö., Uzun, B., Yaylı, M.Ö. and Akgöz, B. (2020), "Size-dependent transverse and longitudinal vibrations of embedded carbon and silica carbide nanotubes by nonlocal finite element method", *Eur. Phys. J. Plus*, **135**(4), 381. https://doi.org/10.1140/epjp/s13360-020-00385-w.

Cuadrado, M., Pernas-Sánchez, J., Artero-Guerrero, J. and Varas, D. (2020), "Model updating of uncertain parameters of carbon/epoxy composite plates using digital image correlation for full-field vibration measurement", *Measurement*, **2020**, 107783. https://doi.org/10.1016/j.measurement.2020.107783.

Deng, Y., Cheng, C., Yang, Y., Peng, Z., Yang, W. and Zhang, W. (2016), "Parametric identification of nonlinear vibration systems via polynomial chirplet transform", *J. Vib. Acoust.*, **138**(5), 051014. https://doi.org/10.1115/1.4033717.

Ebrahimi, F., Barati, M.R. and Civalek, Ö. (2019), "Application of Chebyshev–Ritz method for static stability and vibration analysis of nonlocal microstructure-dependent nanostructures", *Eng. Comput.*, **2019**, 1-12. https://doi.org/10.1007/s00366-019-00742-z.

Ebrahimian, H., Astroza, R. and Conte, J.P. (2015), "Extended Kalman filter for material parameter estimation in nonlinear structural finite element models using direct differentiation method", *Earthq. Eng. Struct. Dyn.*, **44**(10), 1495-1522. https://doi.org/10.1002/eqe.2532.

Erazo, K. and Nagarajaiah, S. (2018), "Bayesian structural identification of a hysteretic negative stiffness earthquake protection system using unscented Kalman filtering", *Struct. Control Health Monit.*, **25**(9), e2203. https://doi.org/10.1002/stc.2203.

Eremin, A., Glushkov, E., Glushkova, N. and Lammering, R. (2015), "Evaluation of effective elastic properties of layered composite fiber-reinforced plastic plates by piezoelectrically induced guided waves and laser Doppler vibrometry", *Compos. Struct.*, **125**, 449-458. https://doi.org/10.1016/j.compstruct.2015.02.029.

Gallina, A., Pieczonka, L., Ambrozinski, L., Packo, P., Nazarko, P., Uhl, T. and Waszczyszyn, Z. (2015), "Analysis of Lamb wave dispersion curve sensitivity to material elastic constants in composites", *Proceedings of the SPIE Smart Structures and Materials Nondestructive Evaluation and Health Monitoring*, California, USA, March.

Gallina, A., Ambrozinski, L., Packo, P., Pieczonka, L., Uhl, T. and Staszewski, W.J. (2017), "Bayesian parameter identification of orthotropic composite materials using Lamb waves dispersion curves measurement", *J. Vib. Control*, **23**(16), 2656-2671. https://doi.org/10.1177/1077546315619264.

Ge, L., Wang, X. and Wang, F. (2014), "Accurate modeling of PZT-induced Lamb wave propagation in structures by using a novel spectral finite element method", *Smart Mater. Struct.*, **23**(9), 095018. https://doi.org/10.1088/0964-1726/23/9/095018.

Giurgiutiu, V. (2005), "Tuned Lamb wave excitation and detection with piezoelectric wafer active sensors for structural health monitoring", *J. Intell. Mater. Syst. Struct.*, **16**(4), 291-305. https://doi.org/10.1177/1045389X05050106.

Giurgiutiu, V. (2007), *Structural Health Monitoring: With Piezoelectric Wafer Active Sensors*, Academic Press, California, USA.

Gogu, C., Haftka, R., Le Riche, R., Molimard, J. and Vautrin, A. (2010), "Introduction to the bayesian approach applied to elastic constants identification", *AIAA J.*, **48**(5), 893-903. https://doi.org/10.2514/1.40922.

Hall, J.S. and Michaels, J.E. (2011), "Model-based parameter estimation for characterizing wave propagation in a homogeneous medium", *Inverse Probl.*, **27**(3), 035002. https://doi.org/10.1088/0266-5611/27/3/035002.

Jaynes, E.T. (2003), *Probability Theory: The Logic of Science*, Cambridge University Press, Cambridge, UK.

Jia, H., Zhang, Z., Liu, H., Dai, F., Liu, Y. and Leng, J. (2019), "An approach based on expectation-maximization algorithm for parameter estimation of Lamb wave signals", *Mech. Syst. Signal Process.*, **120**, 341-355. https://doi.org/10.1016/j.ymssp.2018.10.020.

Lechleiter, A. and Schlasche, J.W. (2017), "Identifying Lamé parameters from time-dependent elastic wave measurements", *Inverse Probl. Sci. Eng.*, **25**(1), 2-26. https://doi.org/10.1080/17415977.2015.1132713.

Lee, F.W., Chai, H.K. and Lim, K.S. (2017), "Characterizing concrete surface notch using Rayleigh wave phase velocity and wavelet parametric analyses", *Constr. Build. Mater.*, **136**, 627-642. https://doi.org/10.1016/j.conbuildmat.2016.08.145.

Liew, K., Lei, Z. and Zhang, L. (2015), "Mechanical analysis of functionally graded carbon nanotube reinforced composites: A review", *Compos. Struct.*, **120**, 90-97. https://doi.org/10.1016/j.compstruct.2014.09.041.

Liu, G., Ma, W. and Han, X. (2002), "An inverse procedure for determination of material constants of composite laminates using elastic waves", *Comput. Methods Appl. Mech. Eng.*, **191**(33), 3543-3554. https://doi.org/10.1016/S0045-7825(02)00292-X.

Lu, J., Zhan, Z., Liu, X. and Wang, P. (2018), "Numerical modeling and model updating for smart laminated structures with viscoelastic damping", *Smart Mater. Struct.*, **27**(7), 075038. https://doi.org/10.1088/1361-665X/aac623.

Lynch, S.M. (2007), *Introduction to Applied Bayesian Statistics and Estimation for Social Scientists*, Springer Science & Business Media, New Jersey, USA.

Ma, T., Zhang, Y. and Huang, X. (2014), "A novel approach for stochastic finite element model updating and parameter estimation", *Proc. Inst. Mech. Eng. C J. Mech. Eng. Sci.*, **228**(18), 3329-3342. https://doi.org/10.1177/0954406214529945.

Morales-Valdez, J., Alvarez-Icaza, L. and Sanchez-Sesma, F.J. (2018), "Shear building stiffness estimation by wave traveling time analysis", *Struct. Control Health Monit.*, **25**(1), e2045. https://doi.org/10.1002/stc.2045.

Murakami, A., Shinmura, H., Ohno, S. and Fujisawa, K. (2018), "Model identification and parameter estimation of elastoplastic constitutive model by data assimilation using the particle filter", *Int. J. Num. Anal. Methods Geomech.*, **42**(1), 110-131. https://doi.org/10.1002/nag.2717.

Nevaranta, N., Parkkinen, J., Lindh, T., Niemelä, M., Pyrhönen, O. and Pyrhönen, J. (2015), "Online identification of a mechanical system in the frequency domain with short-time DFT", **36**(3), 157-165. https://doi.org/10.4173/mic.2015.3.3.

Nichols, J., Link, W., Murphy, K. and Olson, C. (2010), "A Bayesian approach to identifying structural nonlinearity using free-decay response: Application to damage detection in composites", *J. Sound Vib.*, **329**(15), 2995-3007. https://doi.org/10.1016/j.jsv.2010.02.004.

Oliveira, É., Maia, N., Marto, A., Da Silva, R., Afonso, F. and Suleman, A. (2016), "Modal characterization of composite flat plate models using piezoelectric transducers", *Mech. Syst. Signal Process.*, **79**, 16-29. https://doi.org/10.1016/j.ymssp.2016.02.046.

Olivier, A. and Smyth, A.W. (2018), "A marginalized unscented Kalman filter for efficient parameter estimation with applications to finite element models", *Comput. Methods Appl. Mech. Eng.*, **339**, 615-643. https://doi.org/10.1016/j.cma.2018.05.014.

Pabisek, E. and Waszczyszyn, Z. (2015), "Identification of thin

elastic isotropic plate parameters applying guided wave measurement and artificial neural networks", *Mech. Syst. Signal Process.*, **64**, 403-412. https://doi.org/10.1016/j.ymssp.2015.04.007.

Pagnotta, L. (2008), "Recent progress in identification methods for the elastic characterization of materials", *Int. J. Mech.*, **2**(4), 129-140.

Pant, S. (2014), *Lamb Wave Propagation and Material Characterization of Metallic and Composite Aerospace Structures for Improved Structural Health Monitoring (SHM)*, Carleton University Ottawa, Ottawa, Canada.

Pedersen, P., Araujo, A., Soares, C. and Herskovits, J. (2005), "An Inverse Method for Parameter Estimation in Active Laminated Structures", *Proceedings of the 6th World Congresses of Structural and Multidisciplinary Optimization*, Rio de Janeiro, Brazil, May.

Périé, J.N. and Passieux, J.C. (2020), "Special issue on advances in digital image correlation (DIC)", *Adv. Digit. Image Correl.*, **10**(4), 1530. https://doi.org/10.3390/app10041530.

Pirboudaghi, S., Tarinejad, R. and Alami, M.T. (2018), "Damage detection based on system identification of concrete dams using an extended finite element-wavelet transform coupled procedure", *J. Vib. Control*, **24**(18), 4226-4246. https://doi.org/10.1177/1077546317722428.

Pollock, P., Yu, L., Sutton, M., Guo, S., Majumdar, P. and Gresil, M. (2014), "Full-field measurements for determining orthotropic elastic parameters of woven glass-epoxy composites using off-axis tensile specimens", *Exp. Tech.*, **38**(4), 61-71.

Raghavan, A. and Cesnik, C.E. (2005), "Finite-dimensional piezoelectric transducer modeling for guided wave based structural health monitoring", *Smart Mater. Struct.*, **14**(6), 1448. https://doi.org/10.1088/0964-1726/14/6/037.

Rahmatabadi, D., Shahmirzaloo, A., Farahani, M., Tayyebi, M. and Hashemi, R. (2019), "Characterizing the elastic and plastic properties of the multilayered Al/Brass composite produced by ARB using DIC", *Mater. Sci. Eng. A*, **753**, 70-78. https://doi.org/10.1016/j.msea.2019.03.002.

Reed, H., Leckey, C.A., Dick, A., Harvey, G. and Dobson, J. (2018), "A model based bayesian solution for characterization of complex damage scenarios in aerospace composite structures", *Ultrasonics*, **82**, 272-288. https://doi.org/10.1016/j.ultras.2017.09.002.

Réthoré, J., Elguedj, T., Coret, M., Chaudet, P. and Combescure, A. (2013), "Robust identification of elasto-plastic constitutive law parameters from digital images using 3D kinematics", *Int. J. Solids Struct.*, **50**(1), 73-85. https://doi.org/10.1016/j.ijsolstr.2012.09.002.

Sanayei, M., Khaloo, A., Gul, M. and Catbas, F.N. (2015), "Automated finite element model updating of a scale bridge model using measured static and modal test data", *Eng. Struct.*, **102**, 66-79. https://doi.org/10.1016/j.engstruct.2015.07.029.

Sen, S. and Bhattacharya, B. (2018), "Non-Gaussian parameter estimation using generalized polynomial chaos expansion with extended Kalman filtering", *Struct. Safety*, **70**, 104-114. https://doi.org/10.1016/j.strusafe.2017.10.009.

Shao, Q., Younes, A., Fahs, M. and Mara, T.A. (2017), "Bayesian sparse polynomial chaos expansion for global sensitivity analysis", *Comput. Methods Appl. Mech. Eng.*, **318**, 474-496. https://doi.org/10.1016/j.cma.2017.01.033.

Shen, Y. and Giurgiutiu, V. (2016), "Combined analytical FEM approach for efficient simulation of Lamb wave damage detection", *Ultrasonics*, **69**, 116-128. https://doi.org/10.1016/j.ultras.2016.03.019.

Shinozuka, M. and Ghanem, R. (1995), "Structural system identification. II: Experimental verification", *J. Eng. Mech.*, **121**(2), 265-273. https://doi.org/10.1061/(ASCE)0733-9399(1995)121:2(265).

Shirzad-Ghaleroudkhani, N., Mahsuli, M., Ghahari, S.F. and Taciroglu, E. (2018), "Bayesian identification of soil-foundation stiffness of building structures", *Struct. Control Health Monit.*, **25**(3), e2090. https://doi.org/10.1002/stc.2090.

Şimşek, M., Kocatürk, T. and Akbaş, Ş.D. (2013), "Static bending of a functionally graded microscale Timoshenko beam based on the modified couple stress theory", *Compos. Struct.*, **95**, 740-747. https://doi.org/10.1016/j.compstruct.2012.08.036.

Słoński, M. (2014), "Sequential stochastic identification of elastic constants using Lamb waves and particle filters", *Comput. Assist. Methods Eng. Sci.*, **21**(1), 15-26.

Sudret, B. (2008), "Global sensitivity analysis using polynomial chaos expansions", *Reliab. Eng. Syst. Safety*, **93**(7), 964-979. https://doi.org/10.1016/j.ress.2007.04.002.

Tam, J.H., Ong, Z.C., Ismail, Z., Ang, B.C. and Khoo, S.Y. (2017a), "Identification of material properties of composite materials using nondestructive vibrational evaluation approaches: A review", *Mech. Adv. Mater. Struct.*, **24**(12), 971-986. https://doi.org/10.1080/15376494.2016.1196798.

Tam, J.H., Ong, Z.C., Lau, C.L., Ismail, Z., Ang, B.C. and Khoo, S.Y. (2017b), "Identification of material properties of composite plates using Fourier-generated frequency response functions", *Mech. Adv. Mater. Struct.*, **2017**, 1-10. https://doi.org/10.1080/15376494.2016.1196798.

Vignoli, L.L., Savi, M.A., Pacheco, P.M. and Kalamkarov, A.L. (2019), "Comparative analysis of micromechanical models for the elastic composite laminae", *Compos. Part B Eng.*, **174**, 106961. https://doi.org/10.1016/j.compositesb.2019.106961.

Vijayanand, V., Mokhtarishirazabad, M., Peng, J., Wang, Y., Gorley, M., Knowles, D. and Mostafavi, M. (2020), "A novel methodology for estimating tensile properties in a small punch test employing in-situ DIC based deflection mapping", *J. Nucl. Mater.*, **538**, 152260. https://doi.org/10.1016/j.jnucmat.2020.152260.

Vishnuvardhan, J., Krishnamurthy, C. and Balasubramaniam, K. (2007a), "Genetic algorithm based reconstruction of elastic constants of orthotropic fibre-reinforced composite plates from ultrasonic velocity data from a single non-symmetry plane", *Compos. Part B*, **38**, 216-227.

Vishnuvardhan, J., Krishnamurthy, C. and Balasubramaniam, K. (2007b), "Genetic algorithm based reconstruction of the elastic moduli of orthotropic plates using an ultrasonic guided wave single-transmitter-multiple-receiver SHM array", *Smart Mater. Struct.*, **16**(5), 1639. https://doi.org/10.1088/0964-1726/16/5/017.

Warner, J.E. and Hochhalter, J.D. (2016), "Probabilistic damage characterization using the computationally-efficient bayesian approach", NASA Langley Research Center Hampton, USA.

Webersen, M., Johannesmann, S., Düchting, J., Claes, L. and Henning, B. (2018), "Guided ultrasonic waves for determining effective orthotropic material parameters of continuous-fiber reinforced thermoplastic plates", *Ultrasonics*, **84**, 53-62. https://doi.org/10.1016/j.ultras.2017.10.005.

Xie, L., Zhou, Z., Zhao, L., Wan, C., Tang, H. and Xue, S. (2018), "Parameter identification for structural health monitoring with extended Kalman filter considering integration and noise effect", *Appl. Sci.*, **8**(12), 2480. https://doi.org/10.3390/app8122480.

Xu, C., Yang, Z., Qiao, B. and Chen, X. (2020), "A parameter estimation based sparse representation approach for mode separation and dispersion compensation of Lamb waves in isotropic plate", *Smart Mater. Struct.*, **29**(3), 035020. https://doi.org/10.1088/1361-665X/ab6ce7.

Yang, J.N., Pan, S. and Lin, S. (2004). "Identification and tracking of structural parameters with unknown excitations", *Am. Control Conf.*, **5**, 4189-4194. https://doi.org/10.23919/ACC.2004.1383965.

Yuen, K.V. and Ortiz, G.A. (2018), "Multiresolution Bayesian nonparametric general regression for structural model updating", *Struct. Control Health Monit.*, **25**(2), e2077. https://doi.org/10.1002/stc.2077.

Zhang, Q. and Zhao, J. (2013), "Determination of mechanical properties and full-field strain measurements of rock material under dynamic loads", *Int. J. Rock Mech. Mining Sci.*, **60**, 423-439. https://doi.org/10.1016/j.ijrmms.2013.01.005.

Zhang, X., Qiang, B. and Greenleaf, J. (2011), "Comparison of the surface wave method and the indentation method for measuring the elasticity of gelatin phantoms of different concentrations", *Ultrasonics*, **51**(2), 157-164. https://doi.org/10.1016/j.ultras.2010.07.005.

Zhang, F., Xiong, H., Shi, W. and Ou, X. (2016a), "Structural health monitoring of Shanghai Tower during different stages using a Bayesian approach", *Struct. Control Health Monit.*, **23**(11), 1366-1384. https://doi.org/10.1002/stc.1840.

Zhang, X., Gao, R.X., Yan, R., Chen, X., Sun, C. and Yang, Z. (2016b), "Multivariable wavelet finite element-based vibration model for quantitative crack identification by using particle swarm optimization", *J. Sound Vib.*, **375**, 200-216. https://doi.org/10.1016/j.jsv.2016.04.018.

Zhang, F., Yang, Y., Ye, X., Yang, J. and Han, B. (2019), "Structural modal identification and MCMC-based model updating by a Bayesian approach", *Smart Struct. Syst., Int. J.*, **24**(5), 631-639. https://doi.org/10.12989/sss.2019.24.5.631.

Zhou, J., Mita, A. and Mei, L. (2015), "Posterior density estimation for structural parameters using improved differential evolution adaptive Metropolis algorithm", *Smart Struct. Syst., Int. J.*, **15**(3), 735-749. https://doi.org/10.12989/sss.2015.15.3.735.

Zou, F. and Aliabadi, M. (2017), "On modelling three-dimensional piezoelectric smart structures with boundary spectral element method", *Smart Mater. Struct.*, **26**(5), 055015. https://doi.org/10.1088/1361-665X/aa6664.

HJ